taining to steady-state photoinduced aquation or ligand exchange where high concentrations of proton and chloride ion have been present.[14,15,43] Since the species $[PtCl_6]^{3-}$ has been observed to be relatively more stable at high HCl concentrations (conditions closer to the earlier photolysis experiments), the inference appears to be that this catalytic behavior is not restricted to a particular type of platinum(III) entity but is a more general feature, albeit the catalytic efficacy may vary considerably between different species.[5]

**Acknowledgment.** The financial support provided by the Natural Sciences and Engineering Research Council of Canada to W.L.W. and by the North Atlantic Treaty Organization (Project No. 0680/85) is very much appreciated.

**Registry No.** $[PtCl_4]^{2-}$, 13965-91-8; $[PtCl_6]^{2-}$, 16871-54-8; $^{\bullet}OH$, 3352-57-6; H, 12385-13-6; $^{\bullet}CH_2C(CH_3)_2OH$, 5723-74-0.

(43) Dreyer, R.; König, K.; Schmidt, H. *Z. Phys. Chem. (Leipzig)* **1964**, *227*, 257-271.

Contribution from the Inorganic Chemistry Laboratory, South Parks Road, Oxford OX1 3QR, U.K.

# Polyhedral Skeletal Electron Pair Theory of Bare Clusters. 1. Small Silicon Clusters

Tom Slee, Lin Zhenyang, and D. M. P. Mingos*

*Received November 11, 1988*

The polyhedral skeletal electron pair theory, which has proved so successful in rationalizing the structures of ligated clusters, is applied to the structures of small clusters of silicon atoms formed in molecular beams. The PSEPT approach is able to account for many structural features of these small silicon clusters. A number of structures considered earlier as candidates for stable structures of a cluster of given nuclearity are shown to be ruled out by application of the PSEPT approach. Neutral silicon clusters have $2n$ electron pairs. The deltahedral geometries exhibited by boranes would be characterized for silicon atoms by $2n + 1$ electron pairs, and so these geometries are not stable. Small silicon clusters are shown to achieve a stable closed-shell electron configuration with a substantial HOMO–LUMO gap by two mechanisms: oblate distortion from the pseudospherical deltahedron to remove one axially antibonding orbital from the bonding region and capping of a suitable pseudospherical polyhedron. The PSEPT approach also suggests why silicon clusters of nuclearity 4, 6, 7, and 10 are more stable than those of nuclearity 5, 8, and 9.

## Introduction

Ligated clusters have been actively investigated for more than 20 years, and their study can be reasonably described as a mature science. Synthetic procedures have been developed that have resulted in cluster compounds for the majority of transition-metal and main-group atoms, and their structures both in the solid state and in solution have been determined by using X-ray crystallographic and spectroscopic techniques.[1] Furthermore, their structures can be rationalized by using a set of simple electron-counting rules that relate the topology of the structure to the pattern of bonding and nonbonding molecular orbitals generated by a specific three-dimensional arrangement of atoms. This theory, described as the polyhedral skeletal electron pair theory,[2,3] has been underpinned by Stone's tensor surface harmonic theory.[4]

The study of clusters formed in molecular beam experiments or by matrix isolation techniques is a much more recent development.[5] Although the major thrust in this area has been directed toward naked metal clusters, there has also been considerable recent interest in clusters of main-group elements and particularly of semiconductors. The nature of the molecular beam experiments precludes direct structural studies by X-ray and electron diffraction techniques, but fortunately when the clusters are being formed from light atoms very accurate molecular orbital techniques can be used reliably to predict the cluster geometries and stabilities.[6] Such a study has been completed by Raghavachari and his coworkers on silicon clusters $Si_n$ ($n$ = 3–10)[7] following earlier work by other researchers using more approximate techniques.[8]

To date the degree of interaction between researchers in the ligated and beam cluster fields has been limited, and a major aim of this paper is to demonstrate the applicability of the ideas developed for ligated clusters from the polyhedral skeletal electron pair theory to naked silicon clusters formed in molecular beam experiments.

The central feature of the polyhedral skeletal electron pair theory is that particular classes of three-dimensional structures have characteristic closed-shell requirements. For example, deltahedral clusters are characterized by $4n + 2$ valence electrons, e.g., $B_nH_n^{2-}$ ($n$ = 5–12),[3,9a] and three-connected clusters by $5n$ valence electrons, e.g., $C_nH_n$ ($n$ = even, 4–20).[9b] These closed-shell requirements maximize the element–element bonding interactions and create a favorable HOMO–LUMO gap. An important implication of this theory is that if the electron count is changed the structure will distort in such a way as to enlarge the HOMO–LUMO gap and by implication strengthen cluster bonding. For example, in the series $B_nH_n^{2-}$, $B_nH_n^{4-}$, and $B_nH_n^{6-}$ the closo-deltahedral cluster observed in the first structure is progressively opened up in the subsequent nido and arachno structures.[10]

In the silicon clusters, $Si_n$, there are always $4n$ valence electrons, which is two fewer than that required to satisfy the closed-shell requirements for closo deltahedra. Therefore, the principal question to be addressed is as follows: How can the deltahedral structures be distorted to create $2n$ bonding and nonbonding molecular orbitals and a sizeable HOMO–LUMO gap? The success of the polyhedral skeletal electron pair theory (PSEPT) for ligated clusters suggests strongly that such arrangements, if available, will be the most stable for $Si_n$ clusters.

## Skeletal Electrons in Silicon Clusters

Tensor surface harmonic (TSH) theory provides a theoretical framework for constructing qualitatively the molecular orbital manifold of pseudospherical clusters. For *closo*-boranes (other

(1) For a survey, see: Johnson, B. F. G. Ed. *Transition Metal Clusters*; Wiley: Chichester, England, 1980.
(2) (a) Mingos, D. M. P. *Nature Phys. Sci.* **1972**, *236*, 99. (b) Mingos, D. M. P. *Acc. Chem. Res.* **1984**, *17*, 311.
(3) (a) Wade, K. *Adv. Inorg. Chem. Radiochem.* **1976**, *18*, 1. (b) Wade, K. In *Transition Metal Clusters*; Johnson, B. F. G., Ed.; Wiley: Chichester, England, 1980.
(4) (a) Stone, A. J. *Inorg. Chem.* **1981**, *20*, 563. (b) Stone, A. J. *Mol. Phys.* **1980**, *41*, 1339. (c) Stone, A. J. *Polyhedron* **1984**, *3*, 1299.
(5) Several recent journal issues have been devoted to the subject. For example: (a) *Chem. Rev.* **1986**, *86*(3). (b) *Surf. Sci.* **1985**, *156*, Parts 1 and 2. (c) *Ber. Bunsen-Ges. Phys. Chem.* **1984**, *88*, 187–322. (d) *Adv. Chem. Phys.* **1987**, *70*, Parts 1 and 2.
(6) Koutecky, J.; Fantucci, P. *Chem. Rev.* **1986**, *86*, 539.
(7) (a) Raghavachari, K. *J. Chem. Phys.* **1985**, *83*, 3520. (b) Raghavachari, K. *J. Chem. Phys.* **1986**, *84*, 5672. (c) Raghavachari, K.; McMichael Rohlfing, C. *J. Chem. Phys.* **1988**, *89*, 2219.
(8) (a) Pacchioni, G.; Koutecky, J. *J. Chem. Phys.* **1986**, *84*, 3301. (b) Tomanek, D.; Schlüter, M. *Phys. Rev. Lett.* **1986**, *56*, 1055. (c) Tomanek, D.; Schlüter, M. *Phys. Rev. B* **1987**, *36*, 1208. (d) Ballone, P.; Andreoni, W.; Car, R.; Parinello, M. *Phys. Rev. Lett.* **1988**, *60*, 271.
(9) (a) Johnston, R. L.; Mingos, D. M. P. *J. Chem. Soc., Dalton Trans.* **1987**, 647. (b) Johnston, R. L.; Mingos, D. M. P. *J. Organomet. Chem.* **1985**, *280*, 407.
(10) Muetterties, E. L., Ed. *Boron Hydride Chemistry*; Academic Press: New York, 1975.

0020-1669/89/1328-2256$01.50/0 

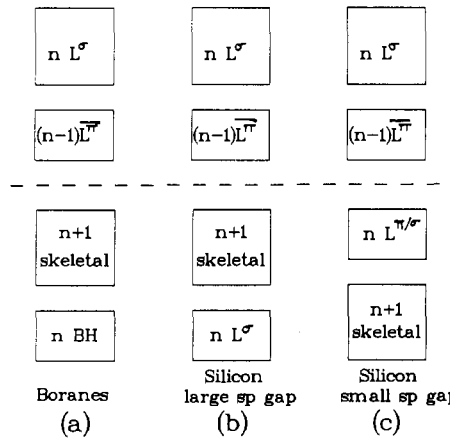


**Figure 1.** Simplified orbital block diagram: (a) deltahedral boranes; (b) silicon clusters, with large s–p energy separation assumed; (c) silicon clusters, with small s–p energy gap assumed.

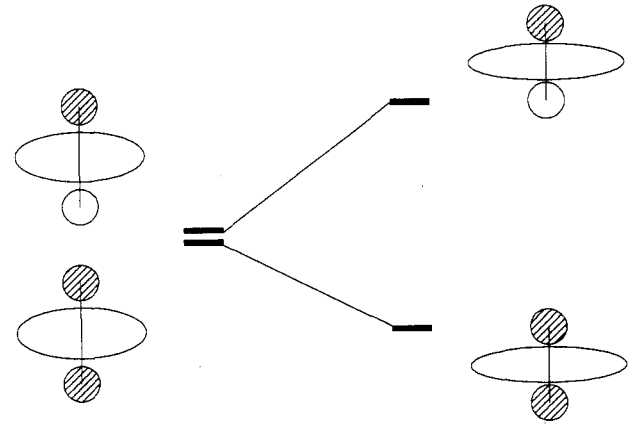

**Figure 2.** Oblate distortion of a pseudospherical cluster. The effect on the axially bonding and antibonding orbitals is shown. The distortion removes one ($P^{\sigma}$) orbital from the bonding region, lowering the appropriate electron-pair count for the cluster by one pair.

than $B_4H_4$), there are predicted to be a total of $n + 1$ accessible (i.e. bonding or nonbonding) skeletal molecular orbitals: one formed from a bonding combination of inward-pointing radial BH frontier orbitals ($S^{\sigma}$) and $n$ $L^{\pi}$ (L = P, D, ...) orbitals formed from tangential $p_{\pi}$ orbitals on the boron. Some of the $\pi$ functions mix with $\sigma$ functions of the same symmetry, but such mixing does not alter the TSH theory conclusions,[4a] as the mixing does not change the number of bonding molecular orbitals; the bonding combinations of $\pi$ and $\sigma$ are occupied and the antibonding combinations unoccupied. In this paper we refer to the bonding combinations of $\pi$ and $\sigma$ functions as $L^{\pi/\sigma}$.

The principal difference between the electronic structures of bare silicon clusters and of boranes arises from the presence of two radial basis functions (s and $p_{\sigma}$) on each silicon atom able to take part in skeletal bonding. The BH bonding orbitals in boranes lie at low energy and so are excluded from the skeletal electron count. The extent of participation of silicon s functions in skeletal bonding depends on the s–p energy separation and on the relative overlap integrals for these functions. Two qualitative possibilities exist, which are shown along with the borane case in Figure 1.

It can be seen from parts a and b of Figure 1 that if the s–p separation were large, silicon clusters would be expected to follow the same electron-counting rules as the deltahedral boranes and to have similar frontier orbitals. The $n$ s functions would be too stable to effectively participate in skeletal bonding. The radial and tangential p orbitals would act in a manner similar to the radial and tangential frontier orbitals of the BH fragment, to generate $L_p^{\sigma}$ and $nL^{\pi/\sigma}$ molecular orbitals.

If, however, the s orbitals were less corelike, they would play an important part in the skeletal bonding. The resulting spectrum of molecular orbitals is represented schematically in Figure 1c. There is one very stable radial $S_{sp}^{\sigma}$ function formed from s and $p_{\sigma}$ functions, followed by $n$ orbitals derived from the tangential $\pi$ functions, $nL^{\pi/\sigma}$. The latter consist of a bonding combination of $\pi$ TSH functions and $\sigma$ TSH functions of the same symmetry. The $n$ occupied frontier orbitals are primarily radial p functions but are hybridized outward by admixture with the s functions, forming $n$ outward-pointing radial functions $L^{\sigma}$. These are different in character from the borane frontier orbitals. In a localized description of the bonding these would hold "lone pairs" at the silicon atoms and be classified as nonbonding. A similar basis for classification has been used successfully for the naked clusters of tin, germanium, and bismuth.[11] The $2n - 1$ antibonding orbitals in Figure 1c are derived from the $L^{\pi}$ TSH functions and from the antiboding combinations of the radial functions (mixed in an antibonding manner with the $\pi$ functions).

Extended Hückel molecular orbital calculations indicate that the behavior of pseudospherical silicon clusters is qualitatively between that depicted in parts b and c of Figure 1. Our calculations indicate that the occupied frontier orbitals have the characteristics of $S^{\sigma}$ and $P^{\sigma}$ outward-pointing radial functions, as expected from Figure 1c, but also that the lowest $n$ orbitals have substantial s atomic orbital character, as expected from Figure 1b. Importantly, both cases are characterized by $2n + 1$ electron pairs: $n + 1$ by analogy with the boranes (which we refer to as standard skeletal bonding orbitals) and a further $n$ $\sigma$ orbitals. The electron-pair count for $Si_n$ is fixed at $2n$, and so such pseudospherical clusters are not expected to represent geometric minima. The cluster must distort in a manner to create the largest HOMO–LUMO gap. Two mechanisms can be proposed to achieve this result.

(1) Small clusters of $D_{nh}$ symmetry, with two nuclei on the principal axis, may distort in an oblate "squashing" mode, the two axial nuclei coming within bonding distance of each other. The effect of such a distortion is illustrated in Figure 2: one radial nonbonding orbital is lowered in energy, while the other is pushed up in energy to become antibonding and thus create a significant HOMO–LUMO gap. More generally, the spherical-to-oblate distortion removes the degeneracy of the $P_{ps}^{\sigma}$ radial set and creates a more strongly bonding $P_{xy}^{\sigma}$ pair and an antibonding $P_z^{\sigma}$ component.

The symmetry characteristics of the distortions from spherical symmetry can be predicted within tensor surface harmonic theory. A necessary requirement for orbitals of angular momentum $L$ to be split by the distortion is that the matrix element $\langle LM|V_{L'M'}|LM\rangle$ not vanish, where $\langle LM|V_{L'M'}|LM\rangle$ is the perturbation to the nuclear–electron potential caused by the distortion and $L'M'$ indicates the symmetry of that distortion in the spherical group.

The selection rules for these matrix elements are well-known from crystal field theory:[12] the requirement is that $L'$ must be even and less than or equal to $2L$. In order to split a set of P spherical harmonic functions, therefore, the distortion must be of D character. The distortion to yield an oblate spheroid is one such distortion, since the axial nuclei move inward as the equatorial nuclei move out. Such a mode would belong to the same irreducible representation as a $d_{z^2}$ function. The energy changes produced by the distortion follow a simple barycenter rule that has been discussed in detail elsewhere.[13] It is significant that a spherical-to-prolate distortion is not a favorable solution to the problem because two antibonding $P_{xy}^{\sigma}$ components would be generated and would favor a $4n - 2$ closed-shell situation.

In summary, an oblate silicon polyhedron is characterized by one $S_{sp}^{\sigma}$ strongly bonding radial MO, $nL^{\pi/\sigma}$ tangential MO's, and $n - 1$ $L_{ps}^{\sigma}$ radial outward-pointing orbitals. This distortion is observed for $Si_4$ (square planar) to $Si_7$ (pentagonal bipyramid),

(11) Johnston, R. L.; Mingos, D. M. P. *J. Organomet. Chem.* **1985**, *280*, 407.

(12) (a) Griffith, J. S. *Theory of Transition Metal Ions*; Cambridge University Press: Cambridge, England, 1961. (b) Silver, B. L. *Irreducible Tensor Methods*; Academic Press: New York, 1976.

(13) Wales, D. J.; Mingos, D. M. P. Submitted for publication.

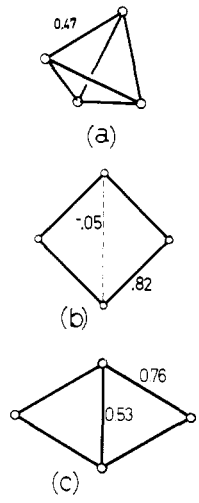


**Figure 3.** Structures for the $Si_4$ cluster, showing the reduced overlap populations between the atoms: (a) $T_d$ symmetry; (b) $D_{4h}$ symmetry; (c) $D_{2h}$ symmetry. Structure c has the lowest energy.

and $Si_8$ undergoes a related distortion.

(2) Within the PSEPT rules, face-capping a polyhedron does not change the skeletal electron count and thereby provides a mechanism for changing the number of tangential bonding molecular orbitals $L^{\pi/\sigma}$ from $n$ to $n-1$. The theoretical basis for this capping principle has been discussed in some detail elsewhere.[14] A capped polyhedron is therefore characterized by $S_{sp}^{\sigma}$, $n-1$ $L^{\pi/\sigma}$, and $nL_{ps}^{\sigma}$ molecular orbitals, capable of accommodating $4n$ electrons.

Where neither mechanism 1 nor mechanism 2 is possible, other distortions of the parent polyhedron will occur to increase the HOMO–LUMO gap. The form these take cannot be simply predicted in a general way.

The silicon clusters $Si_n$, for $n = 4$–10, have been explored by using extended Hückel calculations at model geometries based on the accurate ab initio calculations of Raghavachari and co-workers.[7] The extended Hückel model has well-documented deficiencies but does yield the approximate ordering and form of the molecular orbitals. It is this information we require to investigate the validity of the purely qualitative description given above. For accurate information on individual clusters, we refer to the work of Raghavachari and co-workers, whose extended basis-set calculations, including substantial correlation (Møller–Plesset perturbation theory through fourth order), give energetic and geometric results that we treat as on a par with experimental results.[7] All extended Hückel calculations were carried out with Si–Si nearest-neighbor separations of 2.5 Å. (The $Si_2H_6$ single-bond length is 2.35 Å, and 2.5 Å is a typical cluster bonding distance from Raghavacahari and co-workers' investigations.[7]) The exponent for both 3s and 3p functions was taken as 1.383, and the Coulomb integrals were −17.3 and −9.2 eV, respectively.

We now describe the geometric options open to the $Si_n$ clusters in turn and show how the skeletal electron counting approach enables the observed geometries to be understood.

### $Si_4$

Two possible high-symmetry structures for $Si_4$ are the tetrahedral ($T_d$) and square-planar ($D_{4h}$) arrangements, shown in Figure 3. The polyhedral skeletal electron pair approach predicts that the tetrahedron will have either four or six accessible standard skeletal bonding orbitals.[15] As the band of radial "outward-pointing" orbitals lies at an energy very similar to that of the nonbonding skeletal orbitals, all six skeletal and four radial outward-pointing orbitals must be occupied to yield a significant HOMO–LUMO gap: a total of 10 electron pairs. $Si_4$, with only eight pairs, will thus not be stable in a tetrahedral arrangement.

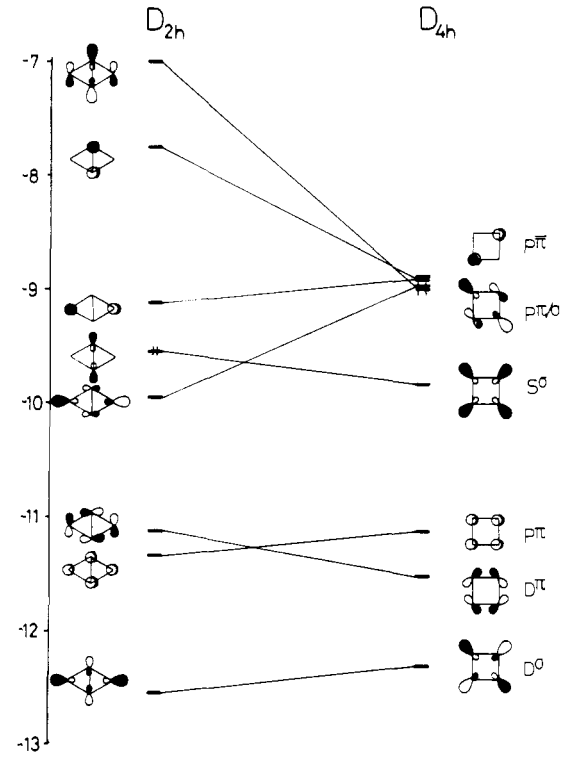


**Figure 4.** Orbital correlation diagram for the $D_{4h}$ to $D_{2h}$ distortion, showing the splitting of the frontier P orbitals and the consequent lowering of the electron-pair count. The HOMOs are indicated by vertical lines representing the electrons and are the $P^{\pi/\sigma}$ set in $D_{4h}$ symmetry and the $S^{\sigma}$ orbital in $D_{2h}$ symmetry.

In the model EHMO calculations we have carried out, it is found to be a triplet with configuration $a_1^2t_2^6t_2^6e^2$. Raghavachari[7b] reports a singlet for the tetrahedron but does find it to be substantially less stable than the rhombus, by 60 kcal/mol.

The square-planar geometry is also a triplet in the EHMO model calculations, as well as in Raghavachari's investigation. In this arrangement, PSEPT predicts five standard skeletal orbitals and four radial outward-pointing orbitals. The oblate distortion (mechanism 1 above) leads to a rhombus (see Figure 3) and to the removal of one orbital from the accessible energy range, leaving eight accessible orbitals for the eight pairs. The rhombus is indeed found to be the minimum energy configuration.

Figure 4 shows an orbital correlation diagram for this distortion. The orbital energy levels of this species contain features that we will see again at higher nuclearities.

At low energy (−22.8 and −17.6 eV; not shown) are an $a_g$ and $e_u$ set, which in TSH classifications are $S^{\sigma}$ and $P_{x,y}^{\pi}$ orbitals, respectively. As mentioned above, the $P^{\pi}$ set contains a substantial contribution from s functions of appropriate symmetry ($P^{\sigma}$), mixed in a bonding fashion, and so are better designated $P^{\pi/\sigma}$. The orbital next higher in energy is a $D^{\sigma}$ orbital, which, in the classification of Figure 1, is a part of the nonbonding band. It may at first sight be surprising that this comes at lower energy than the $D^{\pi}$ orbital, which is the next higher in energy of the standard skeletal bonding orbitals. In fact, the $D^{\sigma}$ orbital, which, if Figure 1 was accurate, would be $D_p^{\sigma}$, is lowered in energy by a mixing in of the vacant $D_s^{\sigma}$ orbital. The presence of a $D^{\sigma}$ orbital lower in energy than the other formally nonbonding orbitals is a feature of many of the small silicon clusters, and the mechanism for energy lowering—the mixing in of an antibonding $D_s^{\sigma}$ orbital—is the same in each case.

The $D^{\pi}$ and remaining $P^{\pi}$ orbitals complete the standard accessible skeletal orbitals, and the $S^{\sigma}$ and $P^{\pi/\sigma}$ sets are the frontier orbitals for this molecule, corresponding to the radial nonbonding orbitals of Figure 1. The HOMO of the $Si_4$ cluster is the doubly degenerate $P^{\pi/\sigma}$ set, which contains two electrons. Only slightly above this set in energy is the $P^{\pi}$ level, which, because of the substantial distortion of the square-planar arrangement from

(14) Mingos, D. M. P.; Forsyth, M. I. *J. Chem. Soc., Dalton Trans.* **1977**, 610.
(15) See ref 4a and: Fowler, P. W. *Polyhedron* **1985**, 2051.

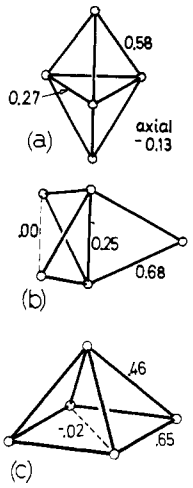


**Figure 5.** Structures for the $Si_5$ cluster, showing the reduced overlap populations between the atoms: (a) $D_{3h}$ symmetry trigonal prism; (b) $D_{3h}$, trigonal prism, related to (a) by an oblate distortion; (c) $C_{4v}$, square pyramid. Structure b has the lowest energy.

spherical symmetry, is also essentially nonbonding.

The distortion of $D$ symmetry to $D_{2h}$ is seen to split the degeneracy of both the $P^{\pi}$ and $P^{\sigma}$ frontier orbital sets. Although the $P^{\sigma}$ splitting is large, the simultaneous splitting of the $P^{\pi}$ set prevents the development of a large HOMO–LUMO gap.

### $Si_5$

Two possible cluster geometries for $Si_5$ are the trigonal bipyramid and the square pyramid, shown in Figure 5. The latter is a nido octahedron and so is expected to have 12 skeletal orbitals (seven from the octahedron, five from the radial nonbonding orbitals) and, therefore, is unfavorable.

The trigonal bipyramid has 11 accessible orbitals: $S^{\sigma}$, 3 $P^{\pi/\sigma}$, $D_0{}^{\sigma}$ $D_{\pm 1}{}^{\pi}$, $S^{\sigma}$, and $P_{0,\pm 1}{}^{\sigma}$. The oblate distortion of this structure leads to a stable structure with 10 accessible orbitals, the $P_0{}^{\sigma}$ frontier orbital being removed from the accessible energy range. The most stable geometry calculated by Raghavachari[7b] shows an axial separation of 2.78 Å. The strength of the driving force behind this distortion is such that the oblate geometry is more stable than the trigonal bipyramid despite the considerable loss of bonding between the equatorial silicon atoms, which separate to 3.26 Å. In our model EHMO calculations the overlap populations between the axial silicon atoms, shown in Figure 5, increase from −0.13 to +0.25 upon oblate distortion, while those between equatorial silicon atoms decrease from 0.27 to 0.00 and that between axial and equatorial atoms increases from 0.58 to 0.68. The capping mechanism (2) above is not available for a cluster with as few atoms as $Si_5$.

### $Si_6$

$Si_6$ has both mechanisms 1 and 2 available to it to produce 12 accessible orbitals and a sizeable HOMO–LUMO gap. the pseudospherical octahedral geometry is calculated to be a triplet, since the number of accessible orbitals is 13. The oblate distortion, which leads to a lengthening of the equatorial bonds, is an essentially isoenergetic process in our model EHMO calculations, the octahedral and $D_{4h}$ geometries differing in energy by only 0.01 eV, but Raghavachari's study[7b] shows this distortion to produce an energy lowering.

The overlap populations shown in Figure 6 provide an explanation as to why the oblate distortion is less favorable for $Si_6$ than for $Si_5$. The axial overlap population increases from −0.18 to +0.20, the axial–equatorial overlap populations remain essentially unchanged, and the equatorial overlap populations between adjacent silicon atoms decrease from 0.53 to −0.09. Despite the relief of destabilizing 1,3-equatorial interactions (an overlap population of −0.18 in the octahedron) the octahedron loses more equatorial bonding in the distortion process than does the trigonal bipyramid.

The second possibility open to $Si_6$ is capping. The bicapped tetrahedron has an electron pair count of 12: six from the skeletal

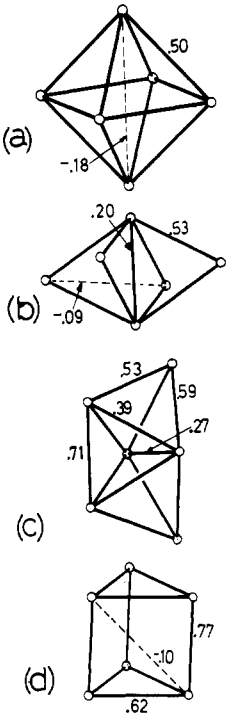


**Figure 6.** Structures for the $Si_6$ cluster, showing the reduced overlap populations between the atoms: (a) $O_h$, octahedron; (b) $D_{4h}$, related to (a) by an oblate distortion; (c) $C_{2v}$, bicapped tetrahedron; (d) $D_{3h}$, trigonal prism. Structure c has the lowest energy.

bonding orbitals of the tetrahedron and six from the radial nonbonding orbitals. The six skeletal molecular orbitals of a bicapped tetrahedron have been discussed in some detail elsewhere[14,16] and are not reproduced here. Raghavachari's calculations[7b] show that there is a flat energy surface for the rearrangement between different face-capped structures, with the intermediate edge-capped geometry being slightly favored, by 1 kcal/mol. These bicapped-tetrahedral structures are substantially lower in energy than the distorted octahedron and so provide the most stable geometry for the $Si_6$ cluster. The bicapped tetrahedron shows a small overlap population (0.27) for the bond that borders both uncapped faces and a large overlap population (0.71) for the bond that borders the two uncapped faces, as shown in Figure 6. Raghavachari's study shows these two bonds to be lengthened and shortened, respectively, compared to the other tetrahedral bonds. The bicapped tetrahedron is a common feature in metal carbonyl chemistry and, for example, has been observed in $Os_6(CO)_{18}$.[17] This molecule is also characterized by six skeletal electron pairs and conforms to the capping principle.[14]

The trigonal prism is another geometry studied by Raghavachari for $Si_6$. This three-connected structure is characterized by nine electron pairs,[9b] so the total count including the outward-pointing radial orbitals is 15. This structure is not expected to be stable. Furthermore, there is no $D$ symmetry distortion that brings two atoms in close contact with each other, so the trigonal prism is not an important structure to consider for $Si_6$.

### $Si_7$

Two possibilities that have the correct electron-pair count of 14 for this cluster are the oblate pentagonal bipyramid and the capped octahedron, shown in Figure 7. In this case the oblate distortion is preferred to the capped polyhedron, and the most stable geometry is the oblate pentagonal bipyramid, a common geometry for bare clusters of several elements. One of the reasons for this is that there is little loss of equatorial bonding accompanying the oblate distortion. The regular pentagonal bipyramid is already oblate, having an axial separation of only 2.63 Å, so

(16) Thomas, K. M.; Mason, R.; Mingos, D. M. P. *J. Am. Chem. Soc.* **1973**, *95*, 3802.
(17) Fantucci, P.; Koutecky, J.; Pacchioni, G. *J. Chem. Phys.* **1984**, *80*, 325.

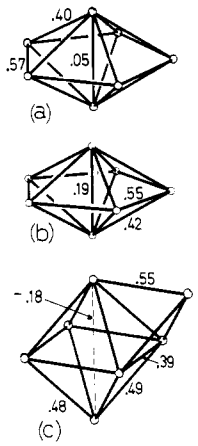


**Figure 7.** Structures for the $Si_7$ cluster, showing the reduced overlap populations between the atoms: (a) $D_{5h}$, pentagonal bipyramid; (b) $D_{5h}$, related to (a) by an oblate distortion; (c) $C_{3v}$, capped octahedron. Structure b has the lowest energy.

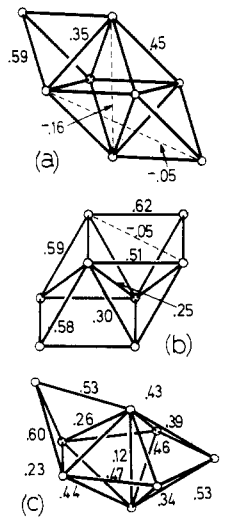


**Figure 8.** Structures for the $Si_8$ cluster, showing the reduced overlap populations between the atoms: (a) $D_{3d}$, bicapped octahedron; (b) $C_{2h}$ sheared cube, related to (a) by an oblate distortion; (c) $C_s$, capped pentagonal bipyramid. Structure b has the lowest energy.

that the axially antibonding $P^\sigma$ orbital is already unoccupied. The distortion further stabilizes the axially bonding $S^\sigma$ orbital.

The third structure found by Raghavachari and Rohlfing[7c] to be a local minimum in the $Si_7$ potential energy surface is a tricapped tetrahedron. That such a structure can be considered electron correct is at first sight surprising, but an extra skeletal orbital can occur when a polyhedron is capped by several atoms, as discussed in the case of $Si_9$ below. This extra orbital, which arises principally from capping-atom $\pi$ orbitals, leads to an electron-pair count of seven skeletal pairs plus seven $\sigma$ pairs, as required. Thus, all three local minima in the $Si_7$ potential surface are electron-correct structures.

### $Si_8$

The discussion above suggests two likely stable geometries for the $Si_8$ cluster: the capped pentagonal bipyramid and a suitably distorted bicapped octahedron. Both are shown in Figure 8. Raghavachari and Rohlfing's calculations[7c] show that the distorted bicapped octahedron is the more stable of the two by 19 kcal/mol. We discuss the two alternatives in turn.

The pentagonal bipyramid is characterized by 15 electrons pairs, and capping would produce the correct electron count of 16 pairs for $Si_8$. As pointed out above, however, even at its regular geometry the pentagonal bipyramid is significantly oblate and the vacant $P_0^\sigma$ ($2a_2''$) orbital is significantly higher in energy than the other two $P^\sigma$ frontier orbitals. Capping does nothing to alter the instability of this (now occupied) orbital, and this is reflected

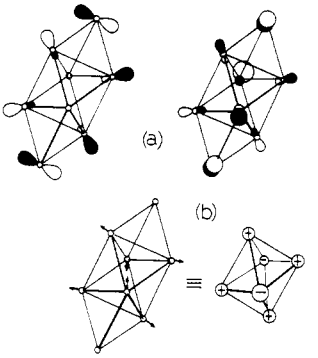


**Figure 9.** (a) Two degenerate $e_u$ orbitals, of $F^{\sigma/\pi}$ type in a TSH construction, which are the frontier orbitals for the bicapped octahedron. (b) Jahn–Teller distortion to the sheared cube (see Figure 7b, along with its relationship to $D$ symmetry behavior in spherical symmetry.

in the long (3.258 Å) axial Si–Si separation found by Raghavachari and Rohlfing.[7c] The capped pentagonal bipyramid is thus not as stable as other formally electron-correct clusters.

The bicapped octahedron is characterized by 15 orbitals, and so $Si_8$ is a triplet at this geometry. The highest occupied orbitals are of $e_u$ symmetry and are shown in Figure 9. Within the TSH model these orbitals, formed by an antibonding combination of capping $p_\pi$ orbitals with $P^\sigma$ orbitals from the octahedron, are of $F^{\sigma/\pi}$ type.

The largest subgroup of $D_{3d}$ in which the $E_u$ representation is split is $C_{2h}$, and the Jahn–Teller distortion leading to this geometry is shown in Figure 9. The distortion involves the breaking of two bonds in the octahedron and the formation of one new bond between two of the previously 1,3-atoms of the octahedron. Figure 9 also shows the relationship of this distortion to the oblate distortions of $Si_4$ through $Si_7$. The two are the same within the TSH model, both having $D$ symmetry.

The most stable geometry found for $Si_8$ thus involves a combination of mechanisms 1 and 2: oblate distortion and capping.

Two other high-symmetry candidate geometries are the tetracapped tetrahedron and the ($D_{2d}$) dodecahedron. Neither of these geometries is electron correct, and our EHMO calculations suggest that both will be Jahn–Teller unstable. It has previously been noted[9a] that the dodecahedron can, in certain main-group clusters such as $B_8Cl_8$, accommodate $n$ skeletal electron pairs as a result of the $\pi$-donor characteristics of the halide ligand. No such ligand is present in the silicon clusters, and hence the dodecahedron is unstable. A local minimum was found by Raghavachari and Rohlfing for a geometry intermediate between the tetracapped tetrahedron and the dodecahedron, a central tetrahedron with two face-capping atoms and one edge bicapped, in $D_{2d}$ symmetry.

### $Si_9$

Raghavachari and Rohlfing[7c] consider only three geometries for $Si_9$. Two of these are shown in Figure 10: the $C_{3v}$ tricapped octahedron and the $D_{3h}$ tricapped trigonal prism. The third geometry is the $C_s$ Jahn–Teller distortion of the tricapped octahedron. The two tricapped structures are predicted by PSEPT to be triplets, but there is an additional subtlety to the electron counting in these structures.

Extended Hückel calculations on the tricapped octahedron show the large HOMO–LUMO gap to occur not between orbitals 16 and 17, as would be expected, but instead between orbitals 17 and 18. The additional orbital added to the electron count of this structure is illustrated in Figure 11. In a fragment decomposition of the cluster into an octahedron plus the three capping atoms, this orbital arises from an antibonding combination of ligand tangential p orbitals of $a_2$ symmetry, but there is little interaction among the capping atoms, and so it is not of significantly higher energy than the other p orbital combinations. There is no bonding orbital of $a_2$ symmetry on the octahedron with which to correlate, and so it is stabilized by combination with an octahedral $a_2$ antibonding orbital and comes into the bonding region.

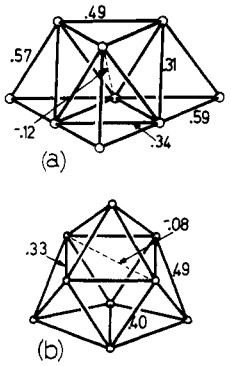


**Figure 10.** Structures for the $Si_9$ cluster, showing the reduced overlap populations between the atoms: (a) $C_{3v}$, tricapped octahedron; (b) $D_{3h}$, tricapped trigonal prism. Neither are minima on the singlet potential energy surface, being Jahn–Teller unstable.

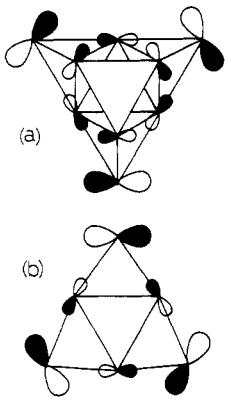


**Figure 11.** Orbitals of (a) the tricapped octahedron and (b) the tricapped trigonal prism, which augment those appropriate for the usual electron-counting rules. Their bonding and antibonding character is discussed in the text.

The same phenomenon has been discussed previously for the tricapped trigonal prism, for which the stable electron count is found to be 19 electron pairs. In this case the combination of tangential p orbitals, shown in Figure 11, is of $a_2'$ symmetry, again finds no match among the bonding orbitals of the trigonal prism, and so is stabilized upon interaction with an antibonding orbital.[14]

The model of silicon cluster bonding presented here suggests that a capped dodecahedron should have the correct electron count for $Si_9$. Such a geometry has not yet been discussed in the literature. The Jahn–Teller distortion of the $C_{3v}$ tricapped octahedron considered by Raghavachari and Rohlfing[7c] creates no significant bonding and so does not have the stability associated with the $Si_8$ Jahn–Teller distortion. The stability of different $Si_9$ structures will be considered in a future publication.

### $Si_{10}$

There are two structures that satisfy the criteria for stability when we reach 10 atoms, and these are shown in Figure 12. The tetracapped octahedron appears at first sight to have three electron pairs too many for the 17 accessible orbitals predicted by the naive application of the rules used above. In fact, the mechanism seen in the $Si_9$ clusters alters the electron count of $Si_{10}$ also.

There is a low-lying $t_1$ set of $P^\pi$ capping orbitals that, just as in the case of $Si_9$, finds no symmetry match among the bonding orbitals of the octahedron. This set of orbitals is stabilized, bringing the electron count for the tetracapped octahedron to 20.

The tetracapped trigonal prism likewise has an electron count of 20 electron pairs: nine from the prism itself, 10 from the radial nonbonding functions, and one capping orbital that finds no symmetry match among the bonding set of the trigonal prism.

Raghavachari and Rohlfing[7c] find these two electron-correct structures to be close in energy, oscillations in their relative energies at various levels of computation precluding a definitive assignment.

Other $Si_{10}$ geometries studied by Raghavachari and Rohlfing include the bicapped tetragonal antiprism, the pentagonal prism, and the pentagonal antiprism. These structures are all electron incorrect and so need not be considered as candidates for stable $Si_{10}$ geometries.

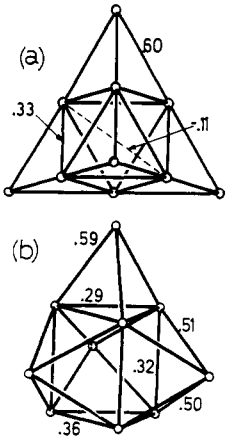


**Figure 12.** Structures for the $Si_{10}$ cluster, showing the reduced overlap populations between the atoms: (a) $T_d$ tetracapped octahedron; (b) $C_{3v}$, tetracapped trigonal prism. Both have closed-shell electronic structures with a sizable HOMO–LUMO gap, and both are minima on the potential energy surface. It is not known which of the two structures is more stable.

### Relative Stability of $Si_n$ Clusters

Both experimental studies[18] and Raghavachari's computational investigations show that the stability of clusters depends crucially on their nuclearity. Raghavachari and Rohlfing show that $Si_n$, $n = 4, 6, 7, 10$, are "locally stable" in the sense that the incremental binding energy $(E_n - (E_{n-1} + E_1))$ is particularly large for these nuclearities. Experimentally, also, these nuclearities are seen to be particularly stable. The PSEPT approach suggests a rationalization of this finding. *The locally stable silicon clusters are those that can form a cluster with correct electron count by capping a pseudospherical cluster or by forming an oblate spheroidal cluster without significant loss of equatorial bonding.*

$Si_4$ forms the oblate rhombus without loss of equatorial bonding. $Si_5$ loses significant equatorial bonding (see above), so that although the oblate geometry is the most stable found for that species $Si_5$ itself is not stable compared with other nuclearities. $Si_6$ forms the bicapped tetrahedron or edge-capped trigonal bipyramid, both of which are electron correct and $Si_7$ forms the oblate pentagonal bipyramid, which retains substantial equatorial bonding in the oblate geometry. $Si_8$ undergoes oblate distortion with the breaking of two "equatorial" bonds, and $Si_9$ finds no electron-correct structure at the geometries studied by Raghavachari and Rohlfing. Finally, $Si_{10}$ has two electron-correct structures open to it.

This rule for the local stability of small silicon cluster nuclearities must be considered provisional while the energy surface of $Si_9$ remains only partially investigated and while $Si_{11}$ remains to be studied.

### Conclusions

The PSEPT approach is able to account for many structural features of small silicon clusters. A number of structures considered as candidates for stable structures of a cluster of given nuclearity can be swiftly ruled out by application of the PSEPT approach. Stable small silicon clusters are shown to achieve a correct electron count by two mechanisms: oblate distortion to remove one axially antibonding orbital from the bonding region and capping of a pseudospherical polyhedron.

**Acknowledgment.** We thank the SERC for providing funding for this project, Dr. David J. Wales for discussions, and Dr. K. Raghavachari for generously providing preprints of his calculations on silicon clusters.

**Registry No.** $Si_4$, 71966-81-9; $Si_5$, 59249-44-4; $Si_6$, 71966-83-1; $Si_7$, 119467-67-3; $Si_8$, 119467-68-4; $Si_9$, 119467-69-5; Si, 7440-21-3.

(18) Heath, J. R.; Liu, Y.; O'Brien, S. C.; Smalley, R. E. *J. Chem. Phys.* **1985**, *83*, 5520.